

# Prompt $J/\psi$ production in hadronic $Z^0$ decays

The OPAL Collaboration

## Abstract

Evidence is presented for the production of prompt  $J/\psi$  mesons (not originating in b-hadron decays) in hadronic  $Z^0$  decays. Using a sample of 3.6 million hadronic events, 24 prompt  $J/\psi$  candidates are identified from their decays into  $e^+e^-$  and  $\mu^+\mu^-$  pairs. The background is estimated to be  $10.2 \pm 2.0$  events. The following branching ratio for prompt  $J/\psi$  production is obtained:

$$Br(Z^0 \rightarrow \text{prompt } J/\psi + X) = (1.9 \pm 0.7 \pm 0.5 \pm 0.5) \cdot 10^{-4},$$

where the first error is statistical, the second systematic and the third error accounts for uncertainties in the prompt  $J/\psi$  production mechanism.

(Submitted to Phys. Lett. B)

# The OPAL Collaboration

G. Alexander<sup>23</sup>, J. Allison<sup>16</sup>, N. Altekamp<sup>5</sup>, K. Ametewee<sup>25</sup>, K.J. Anderson<sup>9</sup>, S. Anderson<sup>12</sup>, S. Arcelli<sup>2</sup>, S. Asai<sup>24</sup>, D. Axen<sup>29</sup>, G. Azuelos<sup>18,a</sup>, A.H. Ball<sup>17</sup>, E. Barberio<sup>26</sup>, R.J. Barlow<sup>16</sup>, R. Bartoldus<sup>3</sup>, J.R. Batley<sup>5</sup>, G. Beaudoin<sup>18</sup>, J. Bechtluft<sup>14</sup>, C. Beeston<sup>16</sup>, T. Behnke<sup>8</sup>, A.N. Bell<sup>1</sup>, K.W. Bell<sup>20</sup>, G. Bella<sup>23</sup>, S. Bentvelsen<sup>8</sup>, P. Berlich<sup>10</sup>, S. Bethke<sup>14</sup>, O. Biebel<sup>14</sup>, V. Blobel<sup>8</sup>, I.J. Bloodworth<sup>1</sup>, J.E. Bloomer<sup>1</sup>, P. Bock<sup>11</sup>, H.M. Bosch<sup>11</sup>, M. Boutemour<sup>18</sup>, B.T. Bouwens<sup>12</sup>, S. Braibant<sup>12</sup>, R.M. Brown<sup>20</sup>, H.J. Burckhart<sup>8</sup>, C. Burgard<sup>27</sup>, R. Bürgin<sup>10</sup>, P. Capiluppi<sup>2</sup>, R.K. Carnegie<sup>6</sup>, A.A. Carter<sup>13</sup>, J.R. Carter<sup>5</sup>, C.Y. Chang<sup>17</sup>, C. Charlesworth<sup>6</sup>, D.G. Charlton<sup>1,b</sup>, D. Chrisman<sup>4</sup>, S.L. Chu<sup>4</sup>, P.E.L. Clarke<sup>15</sup>, I. Cohen<sup>23</sup>, J.E. Conboy<sup>15</sup>, O.C. Cooke<sup>16</sup>, M. Cuffiani<sup>2</sup>, S. Dado<sup>22</sup>, C. Dallapiccola<sup>17</sup>, G.M. Dallavalle<sup>2</sup>, S. De Jong<sup>12</sup>, L.A. del Pozo<sup>8</sup>, K. Desch<sup>3</sup>, M.S. Dixit<sup>7</sup>, E. do Couto e Silva<sup>12</sup>, M. Doucet<sup>18</sup>, E. Duchovni<sup>26</sup>, G. Duckeck<sup>8</sup>, I.P. Duerdoth<sup>16</sup>, J.E.G. Edwards<sup>16</sup>, P.G. Estabrooks<sup>6</sup>, H.G. Evans<sup>9</sup>, M. Evans<sup>13</sup>, F. Fabbri<sup>2</sup>, P. Fath<sup>11</sup>, F. Fiedler<sup>12</sup>, M. Fierro<sup>2</sup>, H.M. Fischer<sup>3</sup>, R. Folman<sup>26</sup>, D.G. Fong<sup>17</sup>, M. Foucher<sup>17</sup>, H. Fukui<sup>24</sup>, A. Fürtjes<sup>8</sup>, P. Gagnon<sup>7</sup>, A. Gaidot<sup>21</sup>, J.W. Gary<sup>4</sup>, J. Gascon<sup>18</sup>, S.M. Gascon-Shotkin<sup>17</sup>, N.I. Geddes<sup>20</sup>, C. Geich-Gimbel<sup>3</sup>, F.X. Gentit<sup>21</sup>, T. Gerasis<sup>20</sup>, G. Giacomelli<sup>2</sup>, P. Giacomelli<sup>4</sup>, R. Giacomelli<sup>2</sup>, V. Gibson<sup>5</sup>, W.R. Gibson<sup>13</sup>, D.M. Gingrich<sup>30,a</sup>, J. Goldberg<sup>22</sup>, M.J. Goodrick<sup>5</sup>, W. Gorn<sup>4</sup>, C. Grandi<sup>2</sup>, E. Gross<sup>26</sup>, M. Gruwé<sup>8</sup>, C. Hajdu<sup>32</sup>, G.G. Hanson<sup>12</sup>, M. Hansroul<sup>8</sup>, M. Hapke<sup>13</sup>, C.K. Hargrove<sup>7</sup>, P.A. Hart<sup>9</sup>, C. Hartmann<sup>3</sup>, M. Hauschild<sup>8</sup>, C.M. Hawkes<sup>5</sup>, R. Hawkings<sup>8</sup>, R.J. Hemingway<sup>6</sup>, G. Herten<sup>10</sup>, R.D. Heuer<sup>8</sup>, M.D. Hildreth<sup>8</sup>, J.C. Hill<sup>5</sup>, S.J. Hillier<sup>1</sup>, T. Hulse<sup>10</sup>, J. Hoare<sup>5</sup>, P.R. Hobson<sup>25</sup>, R.J. Homer<sup>1</sup>, A.K. Honma<sup>28,a</sup>, D. Horváth<sup>32,c</sup>, R. Howard<sup>29</sup>, R.E. Hughes-Jones<sup>16</sup>, D.E. Hutchcroft<sup>5</sup>, P. Igo-Kemenes<sup>11</sup>, D.C. Imrie<sup>25</sup>, M.R. Ingram<sup>16</sup>, A. Jawahery<sup>17</sup>, P.W. Jeffreys<sup>20</sup>, H. Jeremie<sup>18</sup>, M. Jimack<sup>1</sup>, A. Joly<sup>18</sup>, C.R. Jones<sup>5</sup>, G. Jones<sup>16</sup>, M. Jones<sup>6</sup>, R.W.L. Jones<sup>8</sup>, U. Jost<sup>11</sup>, P. Jovanovic<sup>1</sup>, T.R. Junk<sup>8</sup>, D. Karlen<sup>6</sup>, K. Kawagoe<sup>24</sup>, T. Kawamoto<sup>24</sup>, R.K. Keeler<sup>28</sup>, R.G. Kellogg<sup>17</sup>, B.W. Kennedy<sup>20</sup>, B.J. King<sup>8</sup>, J. Kirk<sup>29</sup>, S. Kluth<sup>8</sup>, T. Kobayashi<sup>24</sup>, M. Kobel<sup>10</sup>, D.S. Koetke<sup>6</sup>, T.P. Kokott<sup>3</sup>, S. Komamiya<sup>24</sup>, R. Kowalewski<sup>8</sup>, T. Kress<sup>11</sup>, P. Krieger<sup>6</sup>, J. von Krogh<sup>11</sup>, P. Kyberd<sup>13</sup>, G.D. Lafferty<sup>16</sup>, H. Lafoux<sup>21</sup>, R. Lahmann<sup>17</sup>, W.P. Lai<sup>19</sup>, D. Lanske<sup>14</sup>, J. Lauber<sup>15</sup>, S.R. Lautenschlager<sup>31</sup>, J.G. Layter<sup>4</sup>, D. Lazic<sup>22</sup>, A.M. Lee<sup>31</sup>, E. Lefebvre<sup>18</sup>, D. Lellouch<sup>26</sup>, J. Letts<sup>2</sup>, L. Levinson<sup>26</sup>, C. Lewis<sup>15</sup>, S.L. Lloyd<sup>13</sup>, F.K. Loebinger<sup>16</sup>, G.D. Long<sup>17</sup>, M.J. Losty<sup>7</sup>, J. Ludwig<sup>10</sup>, A. Luig<sup>10</sup>, A. Malik<sup>21</sup>, M. Mannelli<sup>8</sup>, S. Marcellini<sup>2</sup>, C. Markus<sup>3</sup>, A.J. Martin<sup>13</sup>, J.P. Martin<sup>18</sup>, G. Martinez<sup>17</sup>, T. Mashimo<sup>24</sup>, W. Matthews<sup>25</sup>, P. Mättig<sup>3</sup>, W.J. McDonald<sup>30</sup>, J. McKenna<sup>29</sup>, E.A. Mckigney<sup>15</sup>, T.J. McMahon<sup>1</sup>, A.I. McNab<sup>13</sup>, R.A. McPherson<sup>8</sup>, F. Meijers<sup>8</sup>, S. Menke<sup>3</sup>, F.S. Merritt<sup>9</sup>, H. Mes<sup>7</sup>, J. Meyer<sup>27</sup>, A. Michelini<sup>2</sup>, G. Mikenberg<sup>26</sup>, D.J. Miller<sup>15</sup>, R. Mir<sup>26</sup>, W. Mohr<sup>10</sup>, A. Montanari<sup>2</sup>, T. Mori<sup>24</sup>, M. Morii<sup>24</sup>, U. Müller<sup>3</sup>, H.A. Neal<sup>8</sup>, B. Nellen<sup>3</sup>, B. Nijhar<sup>16</sup>, R. Nisius<sup>8</sup>, S.W. O’Neale<sup>1</sup>, F.G. Oakham<sup>7</sup>, F. Odorici<sup>2</sup>, H.O. Ogren<sup>12</sup>, T. Omori<sup>24</sup>, M.J. Oreglia<sup>9</sup>, S. Orito<sup>24</sup>, J. Pálinkás<sup>33,d</sup>, J.P. Pansart<sup>21</sup>, G. Pásztor<sup>32</sup>, J.R. Pater<sup>16</sup>, G.N. Patrick<sup>20</sup>, M.J. Pearce<sup>1</sup>, S. Petzold<sup>27</sup>, P. Pfeifenschneider<sup>14</sup>, J.E. Pilcher<sup>9</sup>, J. Pinfold<sup>30</sup>, D.E. Plane<sup>8</sup>, P. Poffenberger<sup>28</sup>, B. Poli<sup>2</sup>, A. Posthaus<sup>3</sup>, H. Przysiezniak<sup>30</sup>, D.L. Rees<sup>1</sup>, D. Rigby<sup>1</sup>, S.A. Robins<sup>13</sup>, N. Rodning<sup>30</sup>, J.M. Roney<sup>28</sup>, A. Rooke<sup>15</sup>, E. Ros<sup>8</sup>, A.M. Rossi<sup>2</sup>, M. Rosvick<sup>28</sup>, P. Routenburg<sup>30</sup>, Y. Rozen<sup>8</sup>, K. Runge<sup>10</sup>, O. Runolfsson<sup>8</sup>, U. Ruppel<sup>14</sup>, D.R. Rust<sup>12</sup>, R. Rylko<sup>25</sup>, E.K.G. Sarkisyan<sup>23</sup>, M. Sasaki<sup>24</sup>, C. Sbarra<sup>2</sup>, A.D. Schaile<sup>8,e</sup>, O. Schaile<sup>10</sup>, F. Scharf<sup>3</sup>, P. Scharff-Hansen<sup>8</sup>, P. Schenk<sup>4</sup>, B. Schmitt<sup>3</sup>, S. Schmitt<sup>11</sup>, M. Schröder<sup>8</sup>, H.C. Schultz-Coulon<sup>10</sup>, M. Schulz<sup>8</sup>, P. Schütz<sup>3</sup>, W.G. Scott<sup>20</sup>, T.G. Shears<sup>16</sup>, B.C. Shen<sup>4</sup>, C.H. Shepherd-Themistocleous<sup>27</sup>, P. Sherwood<sup>15</sup>, G.P. Siroli<sup>2</sup>, A. Sittler<sup>27</sup>, A. Skillman<sup>15</sup>, A. Skuja<sup>17</sup>, A.M. Smith<sup>8</sup>, T.J. Smith<sup>28</sup>, G.A. Snow<sup>17</sup>, R. Sobie<sup>28</sup>, S. Söldner-Rembold<sup>10</sup>, R.W. Springer<sup>30</sup>, M. Sproston<sup>20</sup>, A. Stahl<sup>3</sup>, M. Starks<sup>12</sup>, M. Steiert<sup>11</sup>, K. Stephens<sup>16</sup>, J. Steuerer<sup>27</sup>, B. Stockhausen<sup>3</sup>, D. Strom<sup>19</sup>, F. Strumia<sup>8</sup>, P. Szymanski<sup>20</sup>, R. Tafirout<sup>18</sup>, S.D. Talbot<sup>1</sup>, S. Tanaka<sup>24</sup>, P. Taras<sup>18</sup>, S. Tarem<sup>22</sup>, M. Tecchio<sup>8</sup>, M. Thiergen<sup>10</sup>, M.A. Thomson<sup>8</sup>, E. von Törne<sup>3</sup>, S. Towers<sup>6</sup>, M. Tscheulin<sup>10</sup>, T. Tsukamoto<sup>24</sup>, E. Tsur<sup>23</sup>, A.S. Turcot<sup>9</sup>, M.F. Turner-Watson<sup>8</sup>, P. Utzat<sup>11</sup>, R. Van Kooten<sup>12</sup>, G. Vasseur<sup>21</sup>, M. Verzocchi<sup>10</sup>, P. Vikas<sup>18</sup>, M. Vincter<sup>28</sup>, E.H. Vokurka<sup>16</sup>, F. Wäckerle<sup>10</sup>, A. Wagner<sup>27</sup>,

C.P. Ward<sup>5</sup>, D.R. Ward<sup>5</sup>, J.J. Ward<sup>15</sup>, P.M. Watkins<sup>1</sup>, A.T. Watson<sup>1</sup>, N.K. Watson<sup>7</sup>, P. Weber<sup>6</sup>,  
P.S. Wells<sup>8</sup>, N. Wermes<sup>3</sup>, J.S. White<sup>28</sup>, B. Wilkens<sup>10</sup>, G.W. Wilson<sup>27</sup>, J.A. Wilson<sup>1</sup>, T. Wlodek<sup>26</sup>,  
G. Wolf<sup>26</sup>, S. Wotton<sup>5</sup>, T.R. Wyatt<sup>16</sup>, S. Yamashita<sup>24</sup>, G. Yekutieli<sup>26</sup>, V. Zacek<sup>18</sup>,

<sup>1</sup>School of Physics and Space Research, University of Birmingham, Birmingham B15 2TT, UK

<sup>2</sup>Dipartimento di Fisica dell' Università di Bologna and INFN, I-40126 Bologna, Italy

<sup>3</sup>Physikalisches Institut, Universität Bonn, D-53115 Bonn, Germany

<sup>4</sup>Department of Physics, University of California, Riverside CA 92521, USA

<sup>5</sup>Cavendish Laboratory, Cambridge CB3 0HE, UK

<sup>6</sup>Ottawa-Carleton Institute for Physics, Department of Physics, Carleton University, Ottawa, Ontario K1S 5B6, Canada

<sup>7</sup>Centre for Research in Particle Physics, Carleton University, Ottawa, Ontario K1S 5B6, Canada

<sup>8</sup>CERN, European Organisation for Particle Physics, CH-1211 Geneva 23, Switzerland

<sup>9</sup>Enrico Fermi Institute and Department of Physics, University of Chicago, Chicago IL 60637, USA

<sup>10</sup>Fakultät für Physik, Albert Ludwigs Universität, D-79104 Freiburg, Germany

<sup>11</sup>Physikalisches Institut, Universität Heidelberg, D-69120 Heidelberg, Germany

<sup>12</sup>Indiana University, Department of Physics, Swain Hall West 117, Bloomington IN 47405, USA

<sup>13</sup>Queen Mary and Westfield College, University of London, London E1 4NS, UK

<sup>14</sup>Technische Hochschule Aachen, III Physikalisches Institut, Sommerfeldstrasse 26-28, D-52056 Aachen, Germany

<sup>15</sup>University College London, London WC1E 6BT, UK

<sup>16</sup>Department of Physics, Schuster Laboratory, The University, Manchester M13 9PL, UK

<sup>17</sup>Department of Physics, University of Maryland, College Park, MD 20742, USA

<sup>18</sup>Laboratoire de Physique Nucléaire, Université de Montréal, Montréal, Quebec H3C 3J7, Canada

<sup>19</sup>University of Oregon, Department of Physics, Eugene OR 97403, USA

<sup>20</sup>Rutherford Appleton Laboratory, Chilton, Didcot, Oxfordshire OX11 0QX, UK

<sup>21</sup>CEA, DAPNIA/SPP, CE-Saclay, F-91191 Gif-sur-Yvette, France

<sup>22</sup>Department of Physics, Technion-Israel Institute of Technology, Haifa 32000, Israel

<sup>23</sup>Department of Physics and Astronomy, Tel Aviv University, Tel Aviv 69978, Israel

<sup>24</sup>International Centre for Elementary Particle Physics and Department of Physics, University of Tokyo, Tokyo 113, and Kobe University, Kobe 657, Japan

<sup>25</sup>Brunel University, Uxbridge, Middlesex UB8 3PH, UK

<sup>26</sup>Particle Physics Department, Weizmann Institute of Science, Rehovot 76100, Israel

<sup>27</sup>Universität Hamburg/DESY, II Institut für Experimental Physik, Notkestrasse 85, D-22607 Hamburg, Germany

<sup>28</sup>University of Victoria, Department of Physics, P O Box 3055, Victoria BC V8W 3P6, Canada

<sup>29</sup>University of British Columbia, Department of Physics, Vancouver BC V6T 1Z1, Canada

<sup>30</sup>University of Alberta, Department of Physics, Edmonton AB T6G 2J1, Canada

<sup>31</sup>Duke University, Dept of Physics, Durham, NC 27708-0305, USA

<sup>32</sup>Research Institute for Particle and Nuclear Physics, H-1525 Budapest, P O Box 49, Hungary

<sup>33</sup>Institute of Nuclear Research, H-4001 Debrecen, P O Box 51, Hungary

<sup>a</sup> and at TRIUMF, Vancouver, Canada V6T 2A3

<sup>b</sup> and Royal Society University Research Fellow

<sup>c</sup> and Institute of Nuclear Research, Debrecen, Hungary

<sup>d</sup> and Department of Experimental Physics, Lajos Kossuth University, Debrecen, Hungary

<sup>e</sup> and Ludwig-Maximilians-Universität, München, Germany

# 1 Introduction

$J/\psi$  mesons are produced at LEP predominantly via b-hadron decays, with a measured branching ratio  $Br(Z^0 \rightarrow J/\psi + X)$  of about  $4.0 \cdot 10^{-3}$  [1–4]. A small number of  $J/\psi$  mesons, and other quarkonium states in general, are expected to be produced in fragmentation processes. The production of  $\Upsilon$  mesons in hadronic  $Z^0$  decays has already been observed [5], but at present only upper limits exist for prompt  $J/\psi$  production [6]. Recent interest in this prompt production mechanism is motivated by the observation at the Tevatron of quarkonium rates larger than expected and the subsequent attempt to explain the excess by novel ‘colour-octet’ production models [7–9]. The production of prompt  $J/\psi$  in  $Z^0$  decays allows a non-trivial test of these models.

Initially, only ‘colour-singlet’ models were considered in estimating the production of prompt  $J/\psi$  mesons. In  $Z^0$  decays, these colour-singlet fragmentation processes consist of ‘c-quark fragmentation’ [10], ‘gluon fragmentation’ [11] and ‘gluon radiation’ [12] contributions (see Fig. 1). The corresponding production rates have been calculated using perturbative QCD. According to these calculations [13], the ‘c-quark fragmentation’ process is dominant, with a branching ratio of:

$$Br(Z^0 \rightarrow J/\psi c\bar{c}) = 0.8 \cdot 10^{-4},$$

including the contribution of cascade decays from  $\psi'$  and  $\chi_c$  states. In the alternative colour-octet models,  $J/\psi$  mesons are first produced in a colour-octet state and then evolve non-perturbatively into colour-singlet states by emission of soft gluons. According to [13], the dominant process in this case is the ‘gluon fragmentation’ process (see Fig. 1), with a branching ratio of:

$$Br(Z^0 \rightarrow J/\psi q\bar{q}) = 1.9 \cdot 10^{-4},$$

including cascade decays (see also alternative calculations in [14]). Both the colour-singlet and colour-octet QCD calculations suffer from potentially large uncertainties since they include only leading terms. In the case of colour-octet models, the total rate depends, in addition, on free parameters adjusted to the Tevatron data [9]. The validity of these production models and rates has yet to be confirmed by experimental measurements.

In this paper, a search for prompt  $J/\psi$  mesons in  $Z^0$  decays is performed.  $J/\psi$  mesons are identified from their decays into  $e^+e^-$  and  $\mu^+\mu^-$  pairs. The outline of this paper is as follows: a brief description of the OPAL detector is presented in Section 2, the main  $J/\psi$  selection criteria are described in Section 3, the prompt  $J/\psi$  selection criteria are discussed in Section 4, and finally, the  $Z^0 \rightarrow$  prompt  $J/\psi + X$  branching ratio is obtained in Section 5.

## 2 The OPAL Detector

The OPAL detector has been described elsewhere [15]. The analysis presented here is based on information from the central tracking system, the lead glass electromagnetic calorimeter and its presampler, the hadron calorimeter and the muon chambers. The tracking system consists of a two layer silicon microstrip vertex detector [16], a vertex drift chamber, a jet chamber and a set of  $z$ -chambers for measurements in the  $z$  direction ( $z$  is the coordinate parallel to the beam axis), all enclosed by a solenoidal magnet coil which produces an axial field of 0.435 T. The main tracking detector is the jet chamber, which has a length of 4 m, a diameter of 3.7 m and which provides up to 159 space points and close to 100% track-finding efficiency for charged tracks in the region  $|\cos\theta| < 0.92$ , where  $\theta$  is the polar angle with respect to the electron beam direction. The momentum resolution can be parametrised as  $(\sigma_{p_t}/p_t)^2 = (0.02)^2 + (0.0015 \cdot p_t)^2$ , where  $p_t$  (in GeV/ $c$ ) is the momentum in the  $x-y$  plane. The jet chamber is also able to perform particle identification by specific energy loss ( $dE/dx$ ) measurements with a resolution of 3.5% for minimum ionising particles with the maximum number of ionisation samples [17].

### 3 Event samples and $J/\psi$ selection

The initial event sample consisted of hadronic  $Z^0$  decays recorded by OPAL in 1990-94 and selected using standard criteria [18]. Tracks were required to satisfy minimum quality cuts as in [19] and only events with at least 7 accepted tracks were considered. The selection efficiency for multihadronic events is  $(98.1 \pm 0.5)\%$ , with a background contamination smaller than 0.1%. After all cuts, a total of 3.6 million hadronic events were selected.

The selection efficiencies were estimated using samples of 2000 Monte Carlo (MC) events simulating each of the processes (see Fig. 1):

$$Z^0 \rightarrow J/\psi c\bar{c}, \quad Z^0 \rightarrow J/\psi q\bar{q}g, \quad Z^0 \rightarrow J/\psi gg, \quad Z^0 \rightarrow J/\psi q\bar{q} \quad \text{and} \quad Z^0 \rightarrow J/\psi g,$$

with the subsequent decay  $J/\psi \rightarrow \ell^+\ell^-$ ,  $\ell$  being either an electron or a muon. In all these processes, the partons were generated using the differential cross-sections provided in [10–13]. In the first three processes,  $J/\psi$  mesons are produced in a colour-singlet state and in the last two processes, in a colour-octet state<sup>1</sup>. Since colour-octet states recombine into colour-singlet states by soft gluon emission, some extra energy is expected around colour-octet states. This extra energy has been neglected in the simulation, but is taken into account later in the discussion of systematic uncertainties. A sample of 4 million MC events containing  $Z^0$  decays and another sample of 90 000 events containing the decay chain  $Z^0 \rightarrow b\bar{b} \rightarrow J/\psi + X$ , with the subsequent decay  $J/\psi \rightarrow \ell^+\ell^-$ , were used to estimate the background to prompt  $J/\psi$  production. Both samples were generated using the JETSET 7.4 MC program [20]. Another background source originates from four-fermion events, namely from the process  $e^+e^- \rightarrow q\bar{q} \ell^+\ell^-$ , where the  $\ell^+\ell^-$  pair results mainly from virtual photon emission. This four-fermion background was estimated using the FERMISV generator [21]. The simulated four-fermion event sample of 20 000 events was equivalent to 20 times the integrated luminosity collected by OPAL. For all MC samples, the parton shower and hadronisation processes were simulated using the JETSET model, with parameter settings as described in [22]. All these samples were processed using the complete OPAL detector simulation program [23].

The lepton identification and  $J/\psi$  selection requirements were the same as in [4]. Lepton candidates were required to satisfy the following acceptance cuts:  $p > 2 \text{ GeV}/c$ , where  $p$  is the track momentum, and  $|\cos\theta| < 0.9$ . In order to ensure a reliable calculation of the lepton pair invariant mass, an accurate polar angle measurement ( $z$  chamber association for barrel tracks, and constraint to the point where the track leaves the jet chamber in the case of forward tracks) was required for all lepton tracks.  $J/\psi$  candidates were selected by demanding two electron or two muon tracks of opposite charge, with an opening angle smaller than  $60^\circ$  and with invariant mass<sup>2</sup> in the range  $2.9\text{--}3.3 \text{ GeV}/c^2$ .

The lepton pair invariant mass distribution obtained after all selection cuts (except the mass cut) is displayed in Fig. 2. The total number of  $J/\psi$  candidates in the mass range  $2.9\text{--}3.3 \text{ GeV}/c^2$  is 741. The fake  $J/\psi$  background can be obtained by counting the number of opposite-sign lepton pairs consisting of an electron and a muon ( $e^\pm\mu^\mp$ ). As discussed in [4], these lepton combinations provide a measurement of the background with a systematic error of 5%. The background calculated in this way amounts to  $230 \pm 18$  events, where the error includes both statistical and systematic contributions. The background-subtracted number of  $J/\psi$  mesons in the data sample is  $N_{J/\psi} = 511 \pm 18$ , where the error results from the background subtraction.

### 4 Selection of prompt $J/\psi$ candidates

Most of the  $J/\psi$  candidates originate from b-hadron decays and are expected to be surrounded by other b-quark decay products and by particles created in the b-quark fragmentation process. Prompt

<sup>1</sup>There is also a colour-octet contribution to the process  $Z^0 \rightarrow J/\psi c\bar{c}$ , but this contribution is negligible [13].

<sup>2</sup>The invariant mass resolution for muon pairs is approximately  $60 \text{ MeV}/c^2$ . For electron pairs, the distribution shows a radiative tail towards low values.

$J/\psi$  mesons are expected to be rather isolated, although the degree of isolation is model dependent (see discussion in the next section). In addition,  $J/\psi$  mesons from b-hadron decays carry the lifetime information of the parent b-hadron, whereas prompt  $J/\psi$  are expected to originate from the primary event vertex. Based on these considerations, the separation of prompt  $J/\psi$  candidates is performed with the help of the following variables:

- The ‘isolation energy’,  $E_{\text{isol}}$ . This energy is defined as the extra energy (sum of track momenta and energy of electromagnetic clusters not associated with tracks), contained within a cone of half-angle  $30^\circ$  around the direction of the reconstructed  $J/\psi$ .
- The ‘decay length significance’,  $L/\sigma_L$ , of the lepton pair. The decay length  $L$  is obtained as the distance in the  $x - y$  plane between the estimated event vertex position and the dilepton decay vertex, using the direction of the reconstructed  $J/\psi$  as a constraint (a more detailed description can be found in [24]). The error in  $L$ ,  $\sigma_L$ , is estimated from the track parameter errors and the uncertainty in the position of the event vertex.

Prompt  $J/\psi$  candidates are selected by imposing the additional cuts:

$$E_{\text{isol}} < 4 \text{ GeV} \quad \text{and} \quad |L|/\sigma_L < 4 .$$

The  $E_{\text{isol}}$  distribution for all  $J/\psi$  candidates is displayed in Fig. 3a, together with the distributions for the fake  $J/\psi$  background and for simulated  $J/\psi$  mesons originating in b-hadron decays. The MC sample is normalised to the number of  $J/\psi$  mesons found in the data after demanding  $L/\sigma_L > 2$ , in order to ensure that the  $J/\psi$  sample originates predominantly from b-hadron decays. An excess of events is observed in Fig. 3a at small values of  $E_{\text{isol}}$ . Furthermore, this excess of events is enhanced at small values of  $L/\sigma_L$  (namely  $|L|/\sigma_L < 4$ ), as shown in Fig. 3b. No excess is observed, on the contrary, in the b-decay enriched sample obtained for  $L/\sigma_L > 4$  (see Fig. 3c). Finally, the invariant mass distribution after all cuts (except the mass cut) is displayed in Fig. 4a. This distribution still shows a peak at the position of the  $J/\psi$  mass, thus indicating that the observed excess of events can be related to a  $J/\psi$  signal.

The total number of prompt  $J/\psi$  candidates in the mass range 2.9–3.3 GeV/ $c^2$  is  $N_{\text{cand}} = 24$ . The background in this mass range originates from the following sources:

- Fake  $J/\psi$  candidates, determined from  $e^\pm \mu^\mp$  combinations. This background amounts to  $2.0 \pm 1.4$  events, the error being mainly statistical (the systematic error is of the order of 5%). Using the MC sample of 4 million  $Z^0$  decays, this background is  $2.7 \pm 1.5$  events, a result compatible with the value quoted above.
- Lepton pairs from four-fermion events. This background has been calculated using the four-fermion simulated sample and amounts to  $1.5 \pm 0.4$  events, the error including statistical (0.3) and systematic (0.2) contributions. This background value includes a small contribution of 0.2 events from resonant  $J/\psi$  production, and in general all higher order corrections to the FERMISV MC discussed in [25]. The systematic error of 0.2 events is equal to the sum of all these corrections as in [25].
- Real  $J/\psi$  candidates originating in b-hadron decays. This background has been calculated using the simulated sample of 90 000 events containing the decay chain  $Z^0 \rightarrow b\bar{b} \rightarrow J/\psi + X$ , and amounts to  $6.7 \pm 1.4$  events. The various contributions to the total error are detailed in Table 1. The  $J/\psi$  momentum spectrum in b-decays (at rest) has been reweighted to match the distribution measured by CLEO [26]. The difference between this spectrum and the spectrum obtained with JETSET is used to calculate the systematic error for this background source. The MC events were generated using the Peterson fragmentation function for b-quarks [27], with an average energy of the primary b-hadron, scaled by the beam energy, of  $\langle x_E \rangle_b = 0.713 \pm 0.012$ , as in [4]. The inclusive b-hadron lifetime  $\tau_b = 1.54 \pm 0.02$  ps [28] has also been used in the event simulation.

The experimental errors on these two quantities have been used to calculate the corresponding systematic errors for the background. Finally a variation of track parameter resolutions as in [4] has been performed to estimate the uncertainties in the modelling by the MC of the  $E_{\text{isol}}$  and  $L/\sigma_L$  quantities.

Error source	Events
normalisation error	0.2
$J/\psi$ spectrum in b-decays	0.8
b-quark fragmentation	0.8
b-quark lifetime	0.1
track parameter resolution	0.5
MC statistics	0.5
Total background uncertainty	1.4

Table 1: *Contributions to the background uncertainty for  $J/\psi$  originating from b-hadron decays.*

The total background is  $N_{\text{bkg}} = 10.2 \pm 2.0$ , and the background-subtracted number of prompt  $J/\psi$  candidates is:

$$N_{\text{prompt}} = N_{\text{cand}} - N_{\text{bkg}} = 13.8 \pm 4.9 \pm 2.0,$$

where the first error is statistical and the second results from the background uncertainty. The probability that the background fluctuates to the observed signal of 24 events is  $2 \cdot 10^{-4}$ . Since most of the background consists of  $b\bar{b}$  events, the background estimate can be further investigated by searching for b-hadrons in the hemisphere opposite to the  $J/\psi$  direction. This search was performed by means of an algorithm which looks for vertices displaced from the estimated event vertex position. These vertices are taken as b-hadron decay candidates if they contain at least 3 tracks, if they are separated from the primary vertex by at least 3 times the uncertainty in the separation distance, and if the output value of an artificial neural network designed to reject non-b background is acceptable. This b-tagging algorithm is described in more detail in [29]. The efficiency of this algorithm applied in the hemisphere opposite to the  $J/\psi$  direction can be estimated using the high purity  $Z^0 \rightarrow b\bar{b}$  data sample obtained by selecting  $J/\psi$  candidates satisfying  $L/\sigma_L > 2$ . The resulting efficiency is  $(40.0 \pm 2.6)\%$ , where the error is statistical. Out of the 24 prompt  $J/\psi$  candidates, 3 are identified by the b-tagging algorithm. This result is compatible with the expected value assuming that the data sample consists of 13.8 prompt  $J/\psi$  and 10.2 background events originating mainly from b-hadron decays as explained above. Using the b-tagging efficiencies obtained from the MC for the signal and the various background sources, this expected value is about 4.7 events. On the contrary, if all candidates originate from b-hadron decays, the expected number of b-tagged events is  $9.1 \pm 0.6$ , and the probability of observing only 3 events is 2.1%.

## 5 Inclusive branching ratio

The fraction of prompt  $J/\psi$  events in  $Z^0$  decays is calculated as follows:

$$\frac{Br(Z^0 \rightarrow \text{prompt } J/\psi + X)}{Br(Z^0 \rightarrow J/\psi + X)} = \frac{N_{\text{prompt}}}{N_{J/\psi}} \cdot \frac{\epsilon_{J/\psi}}{\epsilon_{\text{prompt}}},$$

where  $\epsilon_{J/\psi}$  is the efficiency to select all  $J/\psi$  candidates, and  $\epsilon_{\text{prompt}}$  is the efficiency to select prompt  $J/\psi$  candidates. The efficiency  $\epsilon_{J/\psi}$ , calculated using the b-decay MC, is  $\epsilon_{J/\psi} = 0.230 \pm 0.002$ , where the error is statistical. The small proportion of prompt  $J/\psi$  events in the total  $J/\psi$  sample introduces a negligible correction to  $\epsilon_{J/\psi}$ . The  $\epsilon_{\text{prompt}}$  efficiency depends very significantly on the production

process, as can be seen in Table 2. This dependence is introduced in particular by the isolation cut (see also Fig. 3d). For each process the theoretically predicted branching ratio is reported in Table 2. The average efficiency, obtained by weighting individual efficiencies according to the theoretically expected rates, is  $\epsilon_{\text{prompt}} = 0.146 \pm 0.008$ , where the error is statistical. Prompt  $J/\psi$  mesons may also originate from cascade decays. Assuming that direct  $J/\psi$ ,  $\psi'$  and  $\chi_c$  states are produced with relative abundances 0.5:0.2:0.3 [13], the efficiency is further reduced to  $\epsilon_{\text{prompt}} = 0.129 \pm 0.007$ . This value is used below to calculate the  $Z^0$  branching ratio to prompt  $J/\psi$  events.

Production process	Efficiency no isolation cut	Efficiency isolation cut	$Br(Z^0 \rightarrow \text{prompt } J/\psi + X)$ expected
$Z^0 \rightarrow J/\psi \ c\bar{c}$	$0.262 \pm 0.011$	$0.084 \pm 0.006$	$0.8 \cdot 10^{-4}$ [13]
$Z^0 \rightarrow J/\psi \ q\bar{q}gg$	$0.203 \pm 0.010$	$0.104 \pm 0.007$	$0.2 \cdot 10^{-4}$ [11]
$Z^0 \rightarrow J/\psi \ gg$	$0.215 \pm 0.010$	$0.148 \pm 0.009$	$0.5 \cdot 10^{-6}$ [12]
$Z^0 \rightarrow J/\psi \ q\bar{q}$	$0.221 \pm 0.011$	$0.174 \pm 0.009$	$1.9 \cdot 10^{-4}$ [13]
$Z^0 \rightarrow J/\psi \ g$	$0.273 \pm 0.012$	$0.271 \pm 0.012$	$1.6 \cdot 10^{-7}$ [13]

Table 2: Monte Carlo calculation of  $J/\psi$  selection efficiencies for the various prompt  $J/\psi$  production models. The last column gives the theoretical branching ratio for each process. The errors are statistical.

The following systematic uncertainties have been considered in the calculation of the fraction of prompt  $J/\psi$  events (see Table 3):

- The uncertainties on  $N_{J/\psi}$  and  $N_{\text{prompt}}$  due to the background subtraction were determined as described above.
- Most of the systematic uncertainties on the efficiencies cancel in the ratio  $\epsilon_{J/\psi}/\epsilon_{\text{prompt}}$ . The uncertainty on  $\epsilon_{\text{prompt}}$  due to the extra cuts on  $E_{\text{isol}}$  and  $L/\sigma_L$  was determined by varying the track parameter resolutions, as in [4]. There is in addition an uncertainty related to the MC modelling of the  $E_{\text{isol}}$  energy for colour-octet models, due to soft gluon emission. An indication of this uncertainty can be obtained by comparing the efficiency for the processes  $Z^0 \rightarrow J/\psi \ q\bar{q}$  (with no gluon emission) and  $Z^0 \rightarrow J/\psi \ q\bar{q}gg$  (with the emission of two hard gluons), and is included in the model uncertainty discussed below.
- The prompt  $J/\psi$  selection efficiency has been calculated assuming that  $J/\psi$  mesons decay isotropically. In order to account for the unknown  $J/\psi$  polarization, the efficiency has been recalculated assuming that the angular distribution of leptons from  $J/\psi$  decays is proportional to  $1 + \cos^2 \theta^*$ , where  $\theta^*$  is the emission angle in the  $J/\psi$  rest frame with respect to the  $J/\psi$  direction in the laboratory frame.
- As mentioned before, the efficiency  $\epsilon_{\text{prompt}}$  is reduced if the  $J/\psi$  originates from cascade decays of  $\psi'$  and  $\chi_c$  states. The full difference in efficiency, assuming only direct  $J/\psi$  production, and assuming relative production rates for  $J/\psi$ ,  $\psi'$  and  $\chi_c$  states of 0.5:0.2:0.3, is used to estimate the systematic uncertainty due to these production rates.

Taking into account the statistical and systematic uncertainty, the fraction of prompt  $J/\psi$  events in  $Z^0$  decays is:

$$\frac{Br(Z^0 \rightarrow \text{prompt } J/\psi + X)}{Br(Z^0 \rightarrow J/\psi + X)} = (4.8 \pm 1.7 \pm 1.1)\%.$$

The stability of this result was checked by varying the  $E_{\text{isol}}$  cut between 3 and 5 GeV. No significant variation in the result was observed.



Error source	Contribution
background to $N_{\text{prompt}}$	14.5 %
background to $N_{J/\psi}$	3.5 %
efficiency ratio	7.2 %
polarization	6.3 %
cascade decays	13.5 %
MC statistics	5.5 %
Total systematic error	22.9 %

Table 3: *Summary of systematic uncertainties on the fraction of prompt  $J/\psi$  events in  $Z^0$  decays.*

The momentum distribution of prompt  $J/\psi$  candidates is displayed in Fig. 4b. This distribution is compatible with all models of prompt  $J/\psi$  production except  $Z^0 \rightarrow J/\psi g$ . In this last model, the momentum, scaled by the beam energy, is expected to exceed 0.95 for 90% of the candidates. Since no event is observed in this momentum region, an upper limit of 10% (at 90% CL) can be obtained for the contribution of this process to the total prompt  $J/\psi$  signal.

As explained before, the average efficiency  $\epsilon_{\text{prompt}}$  depends on the theoretically expected rates for each of the production processes, but these calculated rates have large uncertainties. An additional error is therefore included to account for these theoretical uncertainties. This error is calculated as the r.m.s. spread of the efficiencies for the various production models (see Table 2) and amounts to 27.5%. The  $Z^0 \rightarrow J/\psi g$  process has been excluded from the calculation, since both the theoretical branching ratio and the momentum distribution of prompt candidates indicate that its contribution to the total signal is likely to be small.

Taking into account all uncertainties, the fraction of prompt  $J/\psi$  events in  $Z^0$  decays is:

$$\frac{Br(Z^0 \rightarrow \text{prompt } J/\psi + X)}{Br(Z^0 \rightarrow J/\psi + X)} = (4.8 \pm 1.7 \pm 1.1 \pm 1.3)\%,$$

where the first error is statistical, the second systematic, and the third error accounts for model uncertainties. Using the measurement from [4]  $Br(Z^0 \rightarrow J/\psi + X) = (3.9 \pm 0.2 \pm 0.3) \cdot 10^{-3}$ , the following inclusive branching ratio is obtained:

$$Br(Z^0 \rightarrow \text{prompt } J/\psi + X) = (1.9 \pm 0.7 \pm 0.5 \pm 0.5) \cdot 10^{-4}.$$

This branching ratio is in agreement with the theoretical expectation of  $2.9 \cdot 10^{-4}$ , obtained by adding together all production mechanisms. However, the experimental measurement does not exclude the hypothesis that the prompt  $J/\psi$  signal is produced by colour-singlet processes alone. In this case, the measured branching ratio would be  $Br(Z^0 \rightarrow \text{prompt } J/\psi + X) = (2.7 \pm 0.9 \pm 0.4 \pm 0.7) \cdot 10^{-4}$ , to be compared with the theoretical expectation of  $1.0 \cdot 10^{-4}$ . This result is also compatible with the upper limit of  $4 \cdot 10^{-4}$  obtained by DELPHI for colour-singlet processes [6].

## 6 Summary

The production of prompt  $J/\psi$  mesons in hadronic  $Z^0$  decays has been studied using a sample of 3.6 million hadronic  $Z^0$  decays. A total of 511  $J/\psi$  mesons are identified from their decays into  $e^+e^-$  and  $\mu^+\mu^-$  pairs. Prompt  $J/\psi$  candidates are selected by requiring isolation and a production vertex not significantly displaced from the estimated event vertex. The number of prompt candidates is 24, with an estimated background of  $10.2 \pm 2.0$  events. The probability that the background fluctuates to the observed number of 24 events is  $2 \cdot 10^{-4}$ . Assuming that the dominant production mechanism is gluon

fragmentation into colour-octet  $J/\psi$  states, the following measurement of the fraction of prompt  $J/\psi$  events in the total sample is obtained:

$$\frac{Br(Z^0 \rightarrow \text{prompt } J/\psi + X)}{Br(Z^0 \rightarrow J/\psi + X)} = (4.8 \pm 1.7 \pm 1.1 \pm 1.3)\%,$$

corresponding to an inclusive branching ratio of

$$Br(Z^0 \rightarrow \text{prompt } J/\psi + X) = (1.9 \pm 0.7 \pm 0.5 \pm 0.5) \cdot 10^{-4}.$$

In both cases, the first error is statistical, the second systematic and the third error is obtained after consideration of other possible production mechanisms.

## Acknowledgements

We would like to thank P.Cho for useful discussions. We also wish to thank the SL Division for the excellent start-up and performance of the LEP accelerator in the data taking and for their continuing close cooperation with our experimental group. In addition to the support staff at our own institutions we are pleased to acknowledge the  
Department of Energy, USA,  
National Science Foundation, USA,  
Particle Physics and Astronomy Research Council, UK,  
Natural Sciences and Engineering Research Council, Canada,  
Israel Ministry of Science,  
Israel Science Foundation, administered by the Israel Academy of Science and Humanities,  
Minerva Gesellschaft,  
Japanese Ministry of Education, Science and Culture (the Monbusho) and a grant under the Monbusho International Science Research Program,  
German Israeli Bi-national Science Foundation (GIF),  
Direction des Sciences de la Matière du Commissariat à l'Energie Atomique, France,  
Bundesministerium für Bildung, Wissenschaft, Forschung und Technologie, Germany,  
National Research Council of Canada,  
Hungarian Foundation for Scientific Research, OTKA T-016660, and OTKA F-015089.

## References

- [1] ALEPH Collab., D.Buskulic et al., Phys. Lett. **B295** (1992) 396.
- [2] L3 Collab., O.Adriani et al., Phys. Lett. **B317** (1993) 467.
- [3] DELPHI Collab., P.Abreu et al., Phys. Lett. **B341** (1994) 109.
- [4] OPAL Collab., G.Alexander et al., *J/ $\psi$  and  $\psi'$  production in hadronic  $Z^0$  decays*, CERN-PPE/95-153, to be published in Z. Phys. **C**.
- [5] OPAL Collab., G.Alexander et al., Phys. Lett. **B370** (1996) 185.
- [6] DELPHI Collab., P.Abreu et al., Z. Phys. **C69** (1996) 575.
- [7] M.Cacciari et al., Phys. Rev. Lett. **73** (1994) 1586;  
M.Cacciari et al., Phys. Lett. **B356** (1995) 553.
- [8] P.Cho and A.Leibovich, Phys. Rev. **D53** (1996) 150.

- [9] P.Cho and A.Leibovich, *Color-Octet quarkonia production II*, CALT 68-2026, to be published in Phys. Rev. **D**.
- [10] E.Braaten, K.Cheung, T.C.Yuan, Phys. Rev. **D48** (1993) 4230;  
V.Barger, K.Cheung, and W.Y.Keung, Phys. Rev. **D41** (1990) 1541.
- [11] E.Braaten, T.C.Yuan, Phys. Rev. Lett. **71** (1993) 1673;  
K.Hagiwara, et al., Phys. Lett. **B267** (1991) 527, Erratum: Phys. Lett. **B316** (1993) 631.
- [12] J.H.Kühn and H.Schneider, Z. Phys. **C11** (1981) 263;  
W.Y.Keung, Phys. Rev. **D23** (1981) 2072.
- [13] P.Cho, Phys. Lett. **B368** (1996) 171.  
The branching ratio  $Br(Z^0 \rightarrow J/\psi q\bar{q})$  quoted in this paper is  $3.3 \cdot 10^{-4}$ . This value is obtained using the results from [8]. If the more recent results from [9] are used instead, this branching ratio becomes  $1.9 \cdot 10^{-4}$ .
- [14] K.Cheung, W.Y.Keung and T.C.Yuan, Phys. Rev. Lett. **76** (1996) 877.
- [15] OPAL Collab., K.Ahmet et al., Nucl. Instrum. and Meth. **A305** (1991) 275.
- [16] P.Allport et al., Nucl. Instrum. and Meth. **A324** (1993) 34;  
P.Allport et al., Nucl. Instrum. and Meth. **A346** (1994) 476.
- [17] M.Hauschild et al., Nucl. Instrum. and Meth. **A314** (1992) 74.
- [18] OPAL Collab., G.Alexander et al., Z. Phys. **C52** (1991) 175.
- [19] OPAL Collab., P.Acton et al., Z. Phys. **C58** (1993) 523.
- [20] T.Sjöstrand, Comp. Phys. Comm. **82** (1994) 74;  
T.Sjöstrand, JETSET 7.4 Manual, CERN-TH.7112/93.
- [21] J.M.Hilgart, R.Kleiss and F.Le Diberder, Comp. Phys. Comm. **75** (1993) 191.
- [22] OPAL Collab., G.Alexander et al., Z. Phys. **C69** (1996) 543.
- [23] J.Allison et al., Nucl. Instrum. and Meth. **A317** (1991) 47.
- [24] OPAL Collab., R.Akers et al., Z. Phys. **C65** (1995) 17.
- [25] OPAL Collab., G.Alexander et al., *A Study of four-fermion final states with high multiplicity at LEP*, CERN-PPE/96-031, to be published in Phys. Lett. **B**.
- [26] CLEO Collab., R.Balest et al., Phys. Rev. **D52** (1995) 2661.
- [27] C.Peterson et al., Phys. Rev. **D27** (1983) 105.
- [28] L.Montanet et al., Review of Particle Properties, Phys. Rev. **D50** (1994) 1173.
- [29] OPAL Collab., R.Akers et al., Z. Phys. **C66** (1995) 19.

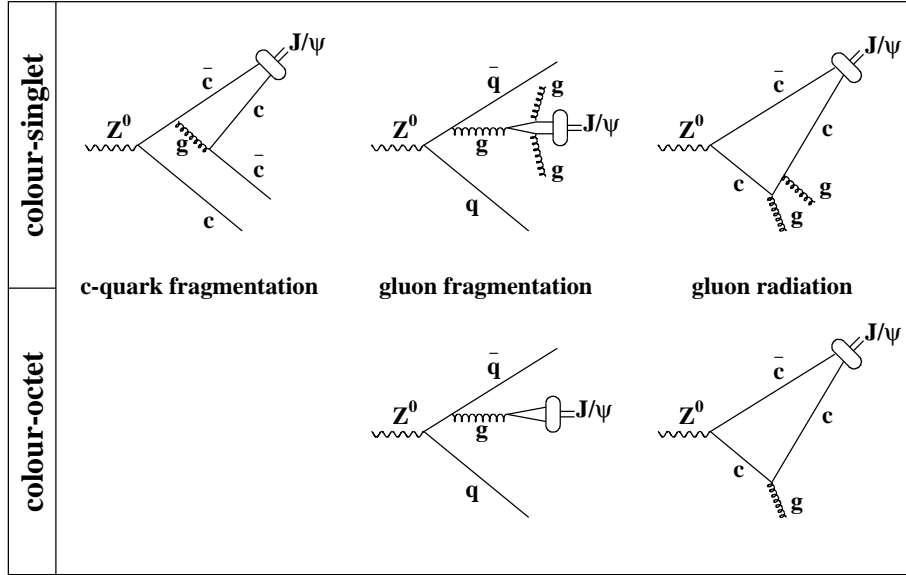


Figure 1: Feynman diagrams for various prompt  $J/\psi$  colour-singlet ( $Z^0 \rightarrow J/\psi c\bar{c}$ ,  $Z^0 \rightarrow J/\psi q\bar{q}g$  and  $Z^0 \rightarrow J/\psi g$ ) and colour-octet ( $Z^0 \rightarrow J/\psi q\bar{q}$  and  $Z^0 \rightarrow J/\psi g$ ) production processes.

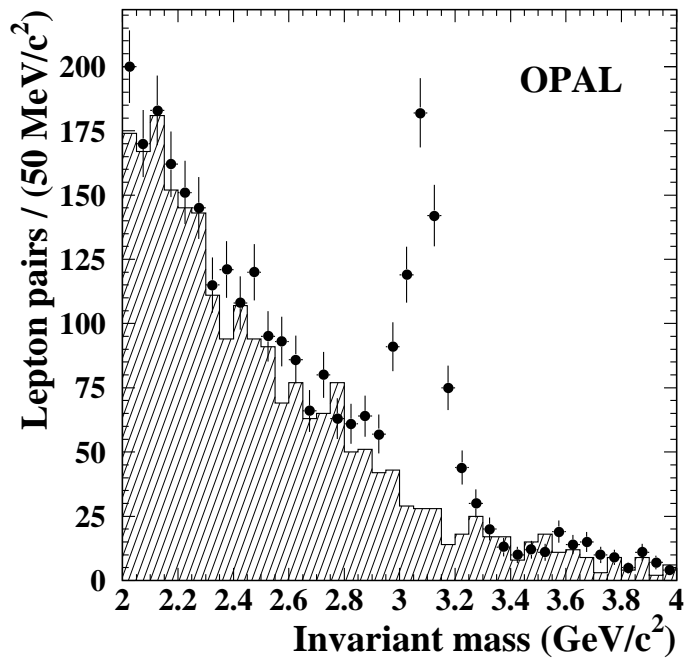


Figure 2: Invariant mass distribution of  $e^+e^-$  and  $\mu^+\mu^-$  pairs. The shaded histogram of  $e^\pm\mu^\mp$  pairs used to calculate the fake  $J/\psi$  background is superimposed.

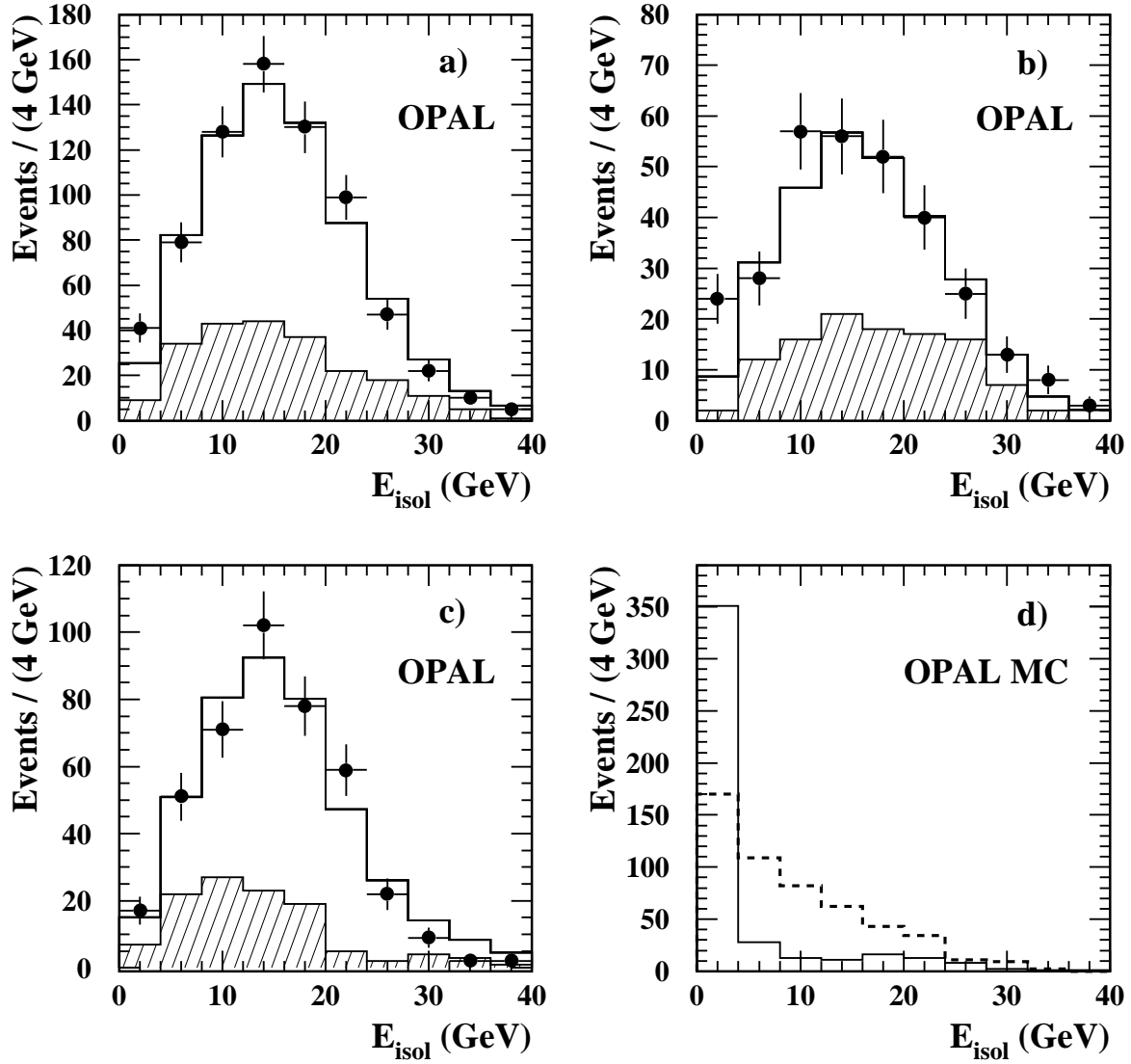


Figure 3:  $E_{\text{isol}}$  distribution for a) all  $J/\psi$  candidates, b) candidates satisfying  $|L|/\sigma_L < 4$  and c) candidates satisfying  $L/\sigma_L > 4$ . The shaded histogram represents the  $E_{\text{isol}}$  distribution for  $e^\pm\mu^\mp$  pairs. The solid line represents the expected distribution for b-quark decays, added to the fake  $J/\psi$  background. The simulated  $E_{\text{isol}}$  distribution for prompt  $J/\psi$  mesons produced according to the processes  $Z^0 \rightarrow J/\psi q\bar{q}$  (solid line) and  $Z^0 \rightarrow J/\psi c\bar{c}$  (dashed line) is shown in d). According to the theoretical calculations reported in Table 2, these two processes are dominant.

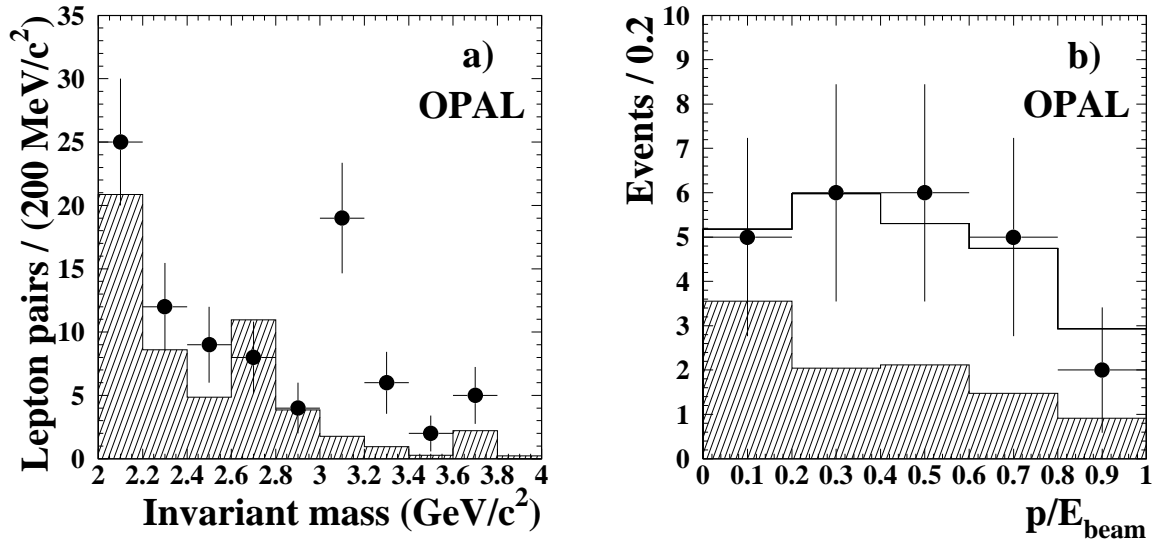


Figure 4: a) Invariant mass distribution of prompt  $J/\psi$  candidates before the invariant mass cut. The shaded histogram includes  $e^\pm\mu^\mp$  pairs used to calculate the fake  $J/\psi$  background and the four-fermion background. b) Momentum distribution of prompt  $J/\psi$  candidates after all cuts (including the mass cut). The shaded histogram includes all background sources and the solid line represents the simulated prompt  $J/\psi$  distribution added to the background.